

**(MARTINGALE) OPTIMAL TRANSPORT AND ANOMALY DETECTION
WITH NEURAL NETWORKS: A PRIMAL-DUAL ALGORITHM**

PIERRE HENRY-LABORDÈRE

ABSTRACT. In this paper, we introduce a primal-dual algorithm for solving (martingale) optimal transportation problems, with cost functions satisfying the twist condition, close to the one that has been used recently for training generative adversarial networks. As some additional applications, we consider anomaly detection and automatic generation of financial data.

1. INTRODUCTION

We introduce a primal-dual algorithm for solving (martingale) optimal transportation problem (in short MOT), potentially large-scale. The martingale optimal transport, first introduced in [2] and in a continuous-time setting in [11], can be defined in a discrete-time setting as the following infinite-dimensional linear program:

$$(1) \quad \text{MK}_c(\mu^1, \mu^2) := \sup_{\mathbb{P} \in \mathcal{M}(\mu^1, \mu^2)} \mathbb{E}^{\mathbb{P}}[c(S_1, S_2)]$$

where $\mathcal{M}(\mu^1, \mu^2) := \{\mathbb{P} \in \mathcal{P}(\mathbb{R}^d, \mathbb{R}^d) : S_1 \stackrel{\mathbb{P}}{\sim} \mu^1, S_2 \stackrel{\mathbb{P}}{\sim} \mu^2, \mathbb{E}^{\mathbb{P}}[S_2|S_1] = S_1\}$ is a weak compact convex set and $\mathcal{P}(\mathbb{R}^d \times \mathbb{R}^d)$ is the set of probability measures on $\mathbb{R}^d \times \mathbb{R}^d$ (or $\mathbb{R}_+^d \times \mathbb{R}_+^d$ if the random variables S_1 and S_2 are interpreted as financial asset prices). A similar definition applies by replacing the supremum over $\mathcal{M}(\mu^1, \mu^2)$ by an infimum. $\text{MK}_c(\mu^1, \mu^2)$ is a number which depends on a cost function $c : \mathbb{R}^d \times \mathbb{R}^d \mapsto \mathbb{R}$ and two marginal distributions μ^1 and μ^2 defined on \mathbb{R}^d . In comparison with the classical OT, we have an additional martingale constraint $\mathbb{E}^{\mathbb{P}}[S_2|S_1] = S_1$ and the linear problem is well-posed if and only if $\mu^1 \leq \mu^2$ in the convex order. In mathematical finance, $\text{MK}_c(\mu^1, \mu^2)$ can then be interpreted as the model-independent arbitrage-free optimal upper bound for a payoff $c(S_1, S_2)$ depending on an asset $S \in \mathbb{R}^d$ evaluated at two maturities $t_1 < t_2$, i.e., $S_1 := S_{t_1}$, $S_2 := S_{t_2}$, which is consistent with the prices (at $t = 0$) of t_1 and t_2 (d -dimensional) European basket options (see [15] for an extensive introduction to MOT and its relevance in arbitrage-free pricing). Our algorithm, described in Section 3, can also be applied to more general linear programs of the form:

$$P_c := \sup_{\mathbb{P} \in \mathcal{M}} \mathbb{E}^{\mathbb{P}}[c(S_1, S_2, \dots, S_n)]$$

where \mathcal{M} is a weak-compact convex subset of $\mathcal{P}((\mathbb{R}^d)^n)$, see for example the multi-marginals (M)OT. However, our algorithm will be applicable only to cost functions satisfying a (martingale) twist condition. Although the extension of our algorithm to this more general setting is straightforward, we prefer for the sake of simplicity to focus on (martingale) OT as defined by (1). Most of the numerical schemes of (M)OT, that we will describe, rely strongly on the dual Monge-Kantorovich

Key words and phrases. (Martingale) optimal transport, Arrow-Hurwicz's algorithm, generative adversarial networks, anomaly detection.

formulation in which $\text{MK}_c(\mu^1, \mu^2)$ can be written as (see [2] for a proof in the context of MOT):

$$(2) \quad \text{MK}_c(\mu^1, \mu^2) := \inf_{u_1 \in L^1(\mu^1), u_2 \in L^1(\mu^2), h \in C_b(\mathbb{R}^d, \mathbb{R}^d)} \mathbb{E}^{\mu^1}[u_1] + \mathbb{E}^{\mu^2}[u_2]$$

such that for all $(s_1, s_2) \in \mathbb{R}^d \times \mathbb{R}^d$

$$(3) \quad u_1(s_1) + u_2(s_2) + h(s_1) \cdot (s_2 - s_1) \geq c(s_1, s_2)$$

By definition, $h(s_1) \cdot (s_2 - s_1) := \sum_{i=1}^d h_i(s_1)(s_2^i - s_1^i)$.

2. NUMERICAL ALGORITHMS: A SHORT OVERVIEW

In this section, we review three numerical algorithms for solving (martingale) optimal transport and highlight their main drawbacks. These algorithms will be compared to our primal-dual method in Section 4.

2.1. Simplex and cutting-plane. The problem (2) (resp. 1) defines a linear program that can be solved using a simplex algorithm. In the context of MOT, this has been explored in [16]. By discretizing the measures μ^1 and μ^2 on a large grid G_∞ in $\mathbb{R}^d \times \mathbb{R}^d$, we obtain a finite-dimensional linear program. Due to the large number $N := \text{card}(G_\infty)$ of linear constraints (3), one can use a cutting-plane algorithm, see [16] for extensive details. This consists in solving the LP program using first a small dimensional grid $G_0 \subset G_\infty$ ($\text{card}(G_0) \ll \text{card}(G_\infty)$). The optimal bound $\text{MK}_c^{(0)}(\mu^1, \mu^2)$ is attained by the dual variables $(u_1^{(0)}, u_2^{(0)}, h^{(0)})$. Then we check on the full grid G_∞ if our optimal dual solution violates the linear constraints (3). The points of G_∞ where the linear constraints are not satisfied, are then added to the grid G_0 , defining a new refined grid G_1 . By construction, we obtain $\text{MK}_c(\mu^1, \mu^2) \geq \text{MK}_c^{(1)}(\mu^1, \mu^2) \geq \text{MK}_c^{(0)}(\mu^1, \mu^2)$ as $G_0 \subset G_1 \subset G_\infty$. The procedure is then iterated until the optimal dual solution $(u_1^{(n)}, u_2^{(n)}, h^{(n)})$ at step (n) satisfies all the constraints on G_∞ for which we can conclude that we have converged towards the true solution. Despite its simplicity, this algorithm could not be extended in large dimension as the number of constraints explodes with the dimension. For example, the complexity of the Hungarian/auction algorithms is $O(N^3)$.

2.2. Entropic relaxation. Another approach is to introduce an entropy penalization (or more generally a f -divergence):

$$\text{MK}_c^\epsilon(\mu^1, \mu^2) := \sup_{\mathbb{P} \in \mathcal{M}(\mu^1, \mu^2)} \mathbb{E}^{\mathbb{P}}[c(S_1, S_2)] - \epsilon H(\mathbb{P} | \mathbb{P}^0)$$

where $H(\mathbb{P} | \mathbb{P}^0) := \mathbb{E}^{\mathbb{P}}[(\ln \frac{d\mathbb{P}}{d\mathbb{P}^0} - 1)]$ is the relative entropy with respect to a prior probability measure $\mathbb{P}^0 \in \mathcal{P}(\mathbb{R}^d \times \mathbb{R}^d)$ and ϵ is a positive parameter taken to be small. In particular, $\lim_{\epsilon \rightarrow 0} \text{MK}_c^\epsilon(\mu^1, \mu^2) = \text{MK}_c(\mu^1, \mu^2)$. The problem $\text{MK}_c^\epsilon(\mu^1, \mu^2)$ can be dualized using the Fenchel-Rockafellar's theorem into a strictly convex optimization problem [16]:

$$(4) \quad \text{MK}_c^\epsilon(\mu^1, \mu^2) := \inf_{u_1 \in L^1(\mu^1), u_2 \in L^1(\mu^2), h \in C_b(\mathbb{R}^d, \mathbb{R}^d)} \mathbb{E}^{\mu^1}[u_1] + \mathbb{E}^{\mu^2}[u_2] + \epsilon \mathbb{E}^{\mathbb{P}^0} [e^{\frac{1}{\epsilon}(c(s_1, s_2) - u_1(s_1) - u_2(s_2) - h(s_1) \cdot (s_2 - s_1))}]$$

2.2.1. *Sinkhorn's algorithm.* By computing the gradients with respect to u_1 , u_2 and h , we obtain the first-order optimality conditions:

$$(5) \quad e^{-\frac{u_1(s_1)}{\epsilon}} \int p_0(s_1, s_2) ds_2 e^{\frac{1}{\epsilon}(c(s_1, s_2) - u_2(s_2) - h(s_1) \cdot (s_2 - s_1))} = \mu^1(s_1)$$

$$(6) \quad e^{-\frac{u_2(s_2)}{\epsilon}} \int p_0(s_1, s_2) ds_1 e^{\frac{1}{\epsilon}(c(s_1, s_2) - u_1(s_1) - h(s_1) \cdot (s_2 - s_1))} = \mu^2(s_2)$$

$$(7) \quad \int p_0(s_1, s_2) ds_2 (s_2 - s_1) e^{\frac{1}{\epsilon}(c(s_1, s_2) - u_2(s_2) - h(s_1) \cdot (s_2 - s_1))} = 0$$

For the sake of simplicity, we have assumed here that \mathbb{P}^0 , μ^1 and μ^2 are absolutely-continuous with respect to the Lebesgue measure. The Sinkhorn algorithm can be then described by the following steps:

(1) Set $n := 1$ and set $u_1^{(0)} := 0$, $u_2^{(0)} := 0$, $h^{(0)} := 0$ for convenience. We approximate the measures μ^1 and μ^2 by Dirac masses supported on N points $(s_1^i)_{1 \leq i \leq N}$ and $(s_2^i)_{1 \leq i \leq N}$.

(2) Compute $u_1^{(n)}(s_1)$ for all $(s_1^i)_{1 \leq i \leq N}$ using

$$e^{-\frac{u_1^{(n)}(s_1)}{\epsilon}} \int p_0(s_1, s_2) ds_2 e^{\frac{1}{\epsilon}(c(s_1, s_2) - u_2^{(n-1)}(s_2) - h^{(n-1)}(s_1) \cdot (s_2 - s_1))} = \mu^1(s_1)$$

(3) Compute $h^{(n)}(s_1)$ for all $(s_1^i)_{1 \leq i \leq N}$ by finding the (unique) zero $\theta \in \mathbb{R}^d$ of

$$h(s_1) := \theta \text{ s.t. } \int p_0(s_1, s_2) ds_2 (s_2 - s_1) e^{\frac{1}{\epsilon}(c(s_1, s_2) - u_2^{(n-1)}(s_2) - \theta \cdot (s_2 - s_1))} = 0$$

(4) Compute $u_2^{(n)}(s_2)$ for all $(s_2^i)_{1 \leq i \leq N}$ using

$$e^{-\frac{u_2^{(n)}(s_2)}{\epsilon}} \int p_0(s_1, s_2) ds_1 e^{\frac{1}{\epsilon}(c(s_1, s_2) - u_1^{(n)}(s_1) - h^{(n)}(s_1) \cdot (s_2 - s_1))} = \mu^2(s_2)$$

(5) Set $n := n + 1$ and iterate steps (2-3-4) up to convergence.

The use of the Sinkhorn algorithm for solving OT problem was introduced in [6] and in [14], [7] in the context of MOT (see also [8] for an application to the construction of arbitrage-free implied volatility surfaces). Again this algorithm does not scale well with the dimension as at each Sinkhorn's iteration, $u_1^{(n)}(s_1)$, $h^{(n)}(s_1)$, $u_2^{(n)}(s_1)$ must be computed on a grid whose the cardinality explodes with the dimension d . The overall complexity is $O(N^2 \ln N)$.

2.3. **and neural networks...** In [19], the optimization (4) is solved by approximating the potentials u_1, u_2 (and h) by some neural networks and then the training is achieved using a stochastic gradient descent algorithm. Similarly, by using Equation (5), the problem (4) can be converted into an equivalent form which involves only the potentials u_2 and h :

$$\begin{aligned} \text{MK}_\epsilon^\epsilon(\mu^1, \mu^2) &:= \inf_{h \in C_b(\mathbb{R}), u_2 \in L^1(\mu^2)} \mathbb{E}^{\mu^2}[u_2] \\ &\quad \epsilon \int \mu^1(ds_1) \ln \int p^0(s_1, s_2) ds_2 e^{\frac{1}{\epsilon}(c(s_1, s_2) - u_2(s_2) - h(s_1) \cdot (s_2 - s_1))} \\ &\quad - \epsilon \int \mu_1(ds_1) (\ln \mu_1(s_1) - 1) \end{aligned}$$

and solve similarly. In [12], instead of using neural networks, the authors make use of an expansion of the dual variables in a reproducing kernel Hilbert space. Despite this algorithm scales properly with the dimension in practise, we will illustrate in our numerical experiments that our computations are unstable when ϵ becomes small. This has been also reported in [12].

2.4. Penalization. In [10], the optimization $\text{MK}_c(\mu^1, \mu^2)$ is approximated by

$$\begin{aligned} \text{MK}_c^\gamma(\mu^1, \mu^2) : &= \inf_{u_1 \in L^1(\mu^1), u_2 \in L^1(\mu^2), h \in C_b(\mathbb{R})} \mathbb{E}^{\mu^1}[u_1] + \mathbb{E}^{\mu^2}[u_2] \\ &+ \gamma \mathbb{E}^{\mathbb{P}^0} [(c(s_1, s_2) - u_1(s_1) - u_2(s_2) - h(s_1)(s_2 - s_1))_+^2] \end{aligned}$$

where γ is a large parameter. This ensures that by taking γ large, the optimal dual solution (u_1^*, u_2^*, h^*) will satisfy the linear constraints (3) and therefore $\lim_{\gamma \rightarrow \infty} \text{MK}_c^\gamma(\mu^1, \mu^2) = \text{MK}_c(\mu^1, \mu^2)$. As above, the potentials u_1, u_2 and h are approximated by some neural networks. This is a classical technique for solving linear programs by penalization and in practise the parameter γ_t is chosen to increase to a large value as the learning parameter η_t , used in the stochastic gradient descent, decreases. In our numerical experiments, we will illustrate that this algorithm is unstable, when the parameter γ is chosen large in order to converge to the true solution. Finally, let us remark that the penalization method can be obtained by replacing the entropy penalization $H(\mathbb{P}|\mathbb{P}^0)$ by the L²-divergence $f(\mathbb{P}|\mathbb{P}^0) := \mathbb{E}^{\mathbb{P}^0} [(\frac{d\mathbb{P}}{d\mathbb{P}^0})^2]$.

3. A PRIMAL-DUAL ALGORITHM

3.1. A saddle-point formulation. For the sake of clarity, we explain our algorithm in the case of the classical OT problem which consists in solving

$$\text{MK}_c(\mu^1, \mu^2) := \sup_{\mathbb{P} \in \mathcal{M}(\mu^1, \mu^2)} \mathbb{E}^{\mathbb{P}}[c(S_1, S_2)]$$

where $\mathcal{M}(\mu^1, \mu^2) := \{\mathbb{P} \in \mathcal{P}(\mathbb{R}^d, \mathbb{R}^d) : S_1 \overset{\mathbb{P}}{\sim} \mu^1, S_2 \overset{\mathbb{P}}{\sim} \mu^2\}$. By introducing the Lagrange multipliers u_1 and u_2 associated to the two marginal constraints, this problem can be written as a minimax (relaxed) optimization problem:

$$\begin{aligned} \text{MK}_c(\mu^1, \mu^2) : &= \inf_{u_1 \in L^1(\mu^1), u_2 \in L^1(\mu^2)} \sup_{\mathbb{P} \in \mathcal{M}_+} \mathbb{E}^{\mu^1}[u_1] + \mathbb{E}^{\mu^2}[u_2] \\ (8) \quad &+ \mathbb{E}^{\mathbb{P}}[c(S_1, S_2) - u_1(S_1) - u_2(S_2)] \end{aligned}$$

where \mathcal{M}_+ denotes the space of positive measures on $\mathbb{R}^d \times \mathbb{R}^d$.

3.2. Using Brenier's theorem.

Definition 3.1 (Twist condition). *A function $c \in C(\mathbb{R}^d \times \mathbb{R}^d)$ differentiable with respect to s_1 is said to be twisted if $\forall s_0 \in \mathbb{R}^d$, the map $s_2 \in \mathbb{R}^d \mapsto \nabla_{s_1} c(s_0, s_2)$ is one-to-one.*

We recall the Brenier theorem (see e.g. [20]):

Theorem 3.2 (Brenier's theorem). *By assuming that μ^1 is absolutely continuous with respect to the Lebesgue measure and the cost function c satisfies the twist condition, the optimal probability measure \mathbb{P}^* , solution of the above saddle-point problem (8), is supported on a unique map $T : \mathbb{R}^d \mapsto \mathbb{R}^d$:*

$$\mathbb{P}^*(ds_1, ds_2) = \mu^1(ds_1)\delta(s_2 - T(s_1))ds_2$$

Note that the constraints $S_1 \overset{\mathbb{P}^*}{\sim} \mu^1$ and $S_2 \overset{\mathbb{P}^*}{\sim} \mu^2$ imply the requirement $T_{\#}\mu^1 = \mu^2$ where $T_{\#}\mu^1$ denotes the push-forward of the measure μ^1 by the map T . T can be characterized as the unique solution of a Monge-Ampère-like equation. More precisely, in the case of the quadratic cost function, T is the gradient of a convex function solution of the Monge-Ampère PDE (see e.g. [20]).

Remark 3.3 (Fréchet-Hoeffding $d = 1$). *Under the (twist) condition $\partial_{s_1 s_2} c \geq 0$ in $d = 1$, the optimal transport can be solved analytically and it is given by the Fréchet-Hoeffding solution:*

$$(9) \quad \text{MK}_c(\mu^1, \mu^2) = \int_0^1 (F_1^{-1}(u) - F_2^{-1}(u))^2 du$$

The map is then $T(s) = F_2^{-1} \circ F_1(s)$ with F_i the cumulative distribution of μ^i .

Under the twist condition, the above minimax optimization (8) can therefore be simplified as

$$(10) \quad \text{MK}_c(\mu^1, \mu^2) := \inf_{u \in L^1(\mu^2)} \sup_{T: \mathbb{R}^d \mapsto \mathbb{R}^d} \mathbb{E}^{\mu^1} [c(S_1, T(S_1)) - u(T(S_1))] + \mathbb{E}^{\mu^2} [u(S_2)]$$

Note that as $S_1 \stackrel{\mathbb{P}^*}{\sim} \mu^1$, the potential u_1 has disappeared and the minimax optimization involves now only the potential $u := u_2$ and the Brenier map T .

3.3. and neural networks... We then approximate the two unknowns $u : \mathbb{R}^d \mapsto \mathbb{R}$ and $T : \mathbb{R}^d \mapsto \mathbb{R}^d$ with two neural networks depending respectively on some weights $\theta \in \mathbb{R}^u$ and $\omega \in \mathbb{R}^t$. $\text{MK}_c(\mu^1, \mu^2)$ can then be approximated by

$$(11) \quad \text{MK}_c^{t,u}(\mu^1, \mu^2) := \min_{\theta \in \mathbb{R}^u} \max_{\omega \in \mathbb{R}^t} \mathbb{E}^{\mu^1} [c(S_1, T_\omega(S_1)) - u_\theta(T_\omega(S_1))] + \mathbb{E}^{\mu^2} [u_\theta(S_2)]$$

In particular, from the universal approximation property of neural networks, we have $\lim_{t,u \rightarrow \infty} \text{MK}_c^{t,u} = \text{MK}_c$.

3.4. Link with Wasserstein generative adversarial networks. The p -Wasserstein distance $\mathcal{W}_p(\mu^1, \mu^2)$ corresponds to an OT problem with a L^p -cost in \mathbb{R}^d , $c(s_1, s_2) := |s_2 - s_1|^p$:

$$(\mathcal{W}_p(\mu^1, \mu^2))^p := \inf_{\mathbb{P} \in \mathcal{M}(\mu^1, \mu^2)} \mathbb{E}^{\mathbb{P}} [|S_2 - S_1|^p]$$

\mathcal{W}_p defines then a distance which metrizes the space $\mathcal{P}(\mathbb{R}^d)$ (see e.g. [20]). If we consider a probability measure μ^{real} in \mathbb{R}^d corresponding to some real data, one would like to reconstruct this density using a mapping $\hat{T} : \mathbb{R}^l \mapsto \mathbb{R}^d$ with $l \ll d$ and such that the push-forward of \hat{T} by a prior density μ^0 supported on \mathbb{R}^l (e.g. an uniform or Gaussian density for the sake of simplicity) is as close as possible to μ^{real} with respect to the Wasserstein distance. The mapping \hat{T} is then chosen to be the solution of

$$\begin{aligned} \text{P} &:= \inf_{\hat{T}: \mathbb{R}^l \mapsto \mathbb{R}^d} \mathcal{W}_p(\mu^1, \mu^2) \\ &= \inf_{\hat{T}: \mathbb{R}^l \mapsto \mathbb{R}^d} \inf_{\mathbb{P} \in \mathcal{M}(\mu^{\text{real}}, \hat{T}_\# \mu^0)} \mathbb{E}^{\mathbb{P}} [|S_2 - S_1|^p] \end{aligned}$$

Note that $H(\hat{T}_\# \mu^0 | \mu^{\text{real}}) = +\infty$ and this is why it is not possible to use the relative entropy as in the case of maximum likelihood estimation. Using the saddle-point formulation of the Wasserstein distance (the L^p -cost satisfies the twist condition) explained in the previous section, this is equivalent to the following minimax optimization:

$$\text{P} = \sup_{u \in L^1(\mu^{\text{real}})} \inf_{\hat{T}: \mathbb{R}^l \mapsto \mathbb{R}^d, T: \mathbb{R}^d \mapsto \mathbb{R}^d} \mathbb{E}^{\mu^{\text{real}}} [c(S_1, T(S_1)) - u(T(S_1))] + \mathbb{E}^{\mu^0} [u(\hat{T}(S_0))]$$

This problem is similar to (10) and therefore as described in Section 3.6, our algorithm copycats the one used for training Wasserstein generative adversarial networks [1] (see also [13]).

Specializing to $p = 1$, we get

$$\text{P} = \sup_{u \in L^1(\mu^{\text{real}})} \inf_{\hat{T}: \mathbb{R}^l \mapsto \mathbb{R}^d, T: \mathbb{R}^d \mapsto \mathbb{R}^d} \mathbb{E}^{\mu^{\text{real}}} [|S_1 - T(S_1)| - u(T(S_1))] + \mathbb{E}^{\mu^0} [u(\hat{T}(S_0))]$$

This should be compared with the dual formulation of the 1-Wasserstein distance used in [1]

$$P = \sup_{u \in \text{Lip}_1} \inf_{\hat{T}: \mathbb{R}^l \rightarrow \mathbb{R}^d} -\mathbb{E}^{\mu^{\text{real}}} [u(S_1)] + \mathbb{E}^{\mu^0} [u(\hat{T}(S_0))]$$

where the supremum is over all the 1-Lipschitz functions. The Lipschitz constraint is enforced in brute force by weight clipping.

Starting from the primal formula of OT and using the Brenier theorem, P can also be written as

$$P = \inf_{\hat{T}: \mathbb{R}^l \rightarrow \mathbb{R}^d, T: \mathbb{R}^d \rightarrow \mathbb{R}^d \text{ s.t. } T_{\#} \mu^{\text{real}} = \hat{T}_{\#} \mu^0} \mathbb{E}^{\mu^{\text{real}}} [c(S_1, T(S_1))]$$

This was done in [4] although the Brenier result is not mentioned. The constraint $T_{\#} \mu^{\text{real}} = \hat{T}_{\#} \mu^0$ is then implemented by adding a penalty term $\gamma D(\cdot | \cdot)$ with γ large:

$$P^\gamma := \inf_{\hat{T}: \mathbb{R}^l \rightarrow \mathbb{R}^d, T: \mathbb{R}^d \rightarrow \mathbb{R}^d} \mathbb{E}^{\mu^{\text{real}}} [c(S_1, T(S_1))] + \gamma D(T_{\#} \mu^{\text{real}} | \hat{T}_{\#} \mu^0)$$

One obtains the Wasserstein-VAE formulation.

3.5. Anomaly detector and data generator. Let us consider some real data generated by a density μ^{real} and let us choose a prior density μ^0 supported on a low-dimensional manifold. As outlined above, we find the density $\hat{T}_{\#} \mu^0$ such that the p -Wasserstein distance $\mathcal{W}_p(\mu^{\text{real}}, \hat{T}_{\#} \mu^0)$ is minimized. Then, a data x_{anomaly} will be considered as an anomaly if $\hat{T}_{\#} \mu^0(x_{\text{anomaly}})$ is below a certain threshold λ :

$$\hat{T}_{\#} \mu^0(x_{\text{anomaly}}) \leq \lambda$$

Similarly, a new data x_{new} can be generated by drawing a random variable Z distributed according to μ^0 and set $x_{\text{new}} = \hat{T}(Z)$.

3.6. Arrow-Hurwicz algorithm: recipe. We simulate μ^1 and μ^2 by Monte-Carlo with N_{MC} paths $(S_1^i, S_2^i)_{1 \leq i \leq N_{\text{MC}}}$ and for large N_{MC} , our optimization (11) consists in solving:

$$\min_{\theta \in \mathbb{R}^u} \max_{\omega \in \mathbb{R}^t} \frac{1}{N_{\text{MC}}} \sum_{i=1}^{N_{\text{MC}}} J_i(\theta, \omega)$$

where

$$J_i(\theta, \omega) := c(S_1^i, T_\omega(S_1^i)) - u_\theta(T_\omega(S_1^i)) + u_\theta(S_2^i)$$

The average functional can be optimized by using a stochastic Arrow-Hurwicz algorithm which consists in doing sequentially the two iterations at each step n : Draw a uniform r.v. $I \in [[1, N_{\text{MC}}]]$ and compute

$$(12) \quad \theta_{n+1} = \theta_n - \eta \nabla_\theta J_I(\theta_n, \omega_n)$$

$$(13) \quad \omega_{n+1} = \omega_n + \eta \nabla_\omega J_I(\theta_{n+1}, \omega_n)$$

where η is a learning parameter. In practise, the gradients are computed by back-propagation where

$$\begin{aligned} \nabla_\theta J_I(\theta, \omega) &= -\nabla_\theta u_\theta(T_\omega(S_1^I)) + \nabla_\theta u_\theta(S_2^I) \\ \nabla_\omega J_I(\theta, \omega) &= (\nabla_{s_2} c(S_1^I, T_\omega(S_1^I)) - \nabla_{s_2} u_\theta(T_\omega(S_1^I))) \cdot \nabla_\omega T_\omega(S_1^I) \end{aligned}$$

We could use also a predictor-corrector scheme:

$$\begin{aligned}\theta_{n+1/2} &= \theta_n - \eta \nabla_{\theta} J_I(\theta_n, \omega_n) \\ \theta_{n+1} &= \theta_n - \eta \nabla_{\theta} J_I(\theta_{n+1/2}, \omega_n) \\ \omega_{n+1/2} &= \omega_n + \eta \nabla_{\omega} J_I(\theta_{n+1}, \omega_n) \\ \omega_{n+1} &= \omega_n + \eta \nabla_{\omega} J_I(\theta_{n+1}, \omega_{n+1/2})\end{aligned}$$

3.7. Convergence. By using one layer for the approximation of the two unknowns T_{ω} and u_{θ} with a linear activation function (a drift can also be included without loss of generality):

$$T(x) := \omega \cdot x, \quad u(x) := \theta^{\dagger} \cdot x, \quad \omega \in M_{p,p}, \quad \theta \in \mathbb{R}^p$$

the problem (11) can be written as

$$(14) \quad \min_{\theta \in \mathbb{R}^p} \max_{\omega \in M_{p,p}} \mathbb{E}^{\mu^1} [c(X, \omega X)] - \theta^{\dagger} \mathbb{E}^{\mu^1} [X] + \theta^{\dagger} \mathbb{E}^{\mu^2} [X]$$

and it is of the form

$$\min_x \max_y y^{\dagger} K x + G(x) + F(y)$$

where K is a linear operator. As shown by [5], the stochastic Arrow-Hurwicz algorithm converges if F is concave, G is convex and $\|K\| \eta^2 < 1$. Our program (14) is clearly convex in θ as being linear and is concave in ω if and only if $D_{s_2}^2 c \leq 0$. This implies that our algorithm converges (in the case of one layer), if we impose that $D_{s_2}^2 c \leq 0$. Additionally, we should have that c satisfies the twist condition as we have used the Brenier theorem.

Let us remark that if we consider the new cost function $\bar{c}(s_1, s_2) = c(s_1, s_2) - U(s_2)$, then we have for all $U \in L^1(\mu^2)$:

$$\text{MK}_{\bar{c}}(\mu^1, \mu^2) + \mathbb{E}^{\mu^2} [U(S_2)] = \text{MK}_c(\mu^1, \mu^2)$$

Using this property, we can apply our algorithm to the cost function \bar{c} where U is chosen such that¹

$$D_{s_2}^2 \bar{c} = D_{s_2}^2 c - D_{s_2}^2 U(s_2) \leq 0, \quad \forall (s_1, s_2) \in \mathbb{R}^d \times \mathbb{R}^d$$

Example 3.4. For $c(x, y) = -(x - y)^2$, we can take $U(y) = 0$. For $c(x, y) = (x + y)^2$, we can take $U(y) = 2y^2$.

Using the result in [5], we conclude:

Proposition 3.5 (Convergence). *Let us assume that c satisfies the twist condition and $D_{s_2}^2 c - D_{s_2}^2 U(s_2) \leq 0$ for some twice differentiable function U in $L^1(\mu^2)$, then the Arrow-Hurwicz algorithm (with one layer) (12-13) converges for η small enough.*

Note that a similar conclusion appears if we expand T_{ω} and u_{θ} in terms of a reproducing kernel Hilbert space.

¹We are grateful to our master students Y. Chen and F. Jiang at Ecole Polytechnique for pointing to us this remark.

3.8. The case of MOT. For $d = 1$, under the (martingale) twist condition $\partial_{s_1} \partial_{s_2}^2 c \geq 0$, the optimal probability measure \mathbb{P}^* is shown to be supported not on a single map T but on two maps $T_d(x) \leq x \leq T_u(x)$ [3, 17]:

$$\mathbb{P}^*(s_1, s_2) = q(s_1)\delta(s_2 - T_u(s_1)) + (1 - q(s_1))\delta(s_2 - T_d(s_1))$$

This leads to the following minimax optimization:

$$\begin{aligned} \text{MK}_c(\mu^1, \mu^2) := & \inf_{u \in L^1(\mu^2), h \in C^0(\mathbb{R}^d, [0,1])} \sup_{T_u: \mathbb{R} \rightarrow \mathbb{R}, T_d: \mathbb{R} \rightarrow \mathbb{R}, q: \mathbb{R} \rightarrow [0,1]} \\ & \mathbb{E}^{\mu^1} [q(S_1)(c(S_1, T_u(S_1)) - u(T_u(S_1)) - h(S_1)(T_u(S_1) - S_1)) \\ & + (1 - q(S_1))(c(S_1, T_d(S_1)) - u(T_d(S_1)) - h(S_1)(T_d(S_1) - S_1))] + \mathbb{E}^{\mu^2} [u(S_2)] \end{aligned}$$

Note that the martingale condition leads explicitly to $q(x) := \frac{x - T_d(x)}{T_u(x) - T_d(x)}$ but we do not use this equation in order to preserve the concavity-convexity property with respect to the neural network weights (in the case of one layer). The algorithm is then similar to the one presented for OT except that now we have five (instead of two) neural networks for the potentials h, u, q and the two maps T_u and T_d .

For $d \geq 2$, one can characterize the cost functions for which the optimal probability measure \mathbb{P}^* is supported on n maps T_i [9]. The above optimization becomes therefore:

$$\begin{aligned} \text{MK}_c(\mu^1, \mu^2) := & \inf_{u \in L^1(\mu^2), h \in C^0(\mathbb{R}^d, [0,1])} \sup_{(T_i)_{1 \leq i \leq n}: \mathbb{R}^d \rightarrow \mathbb{R}^d, q_i: \mathbb{R}^d \rightarrow [0,1]} \\ & \mathbb{E}^{\mu^1} [q_i(S_1)(c(S_1, T_i(S_1)) - u(T_i(S_1)) - h(S_1)(T_i(S_1) - S_1))] + \mathbb{E}^{\mu^2} [u(S_2)] \end{aligned}$$

where $q_n := 1 - \sum_{i=1}^{n-1} q_i$. In practise, the number of maps n can be seen as an hyperparameter that can be optimized.

4. NUMERICAL EXAMPLES

4.1. OT in $d = 1$. We first check our algorithm described in Section 3.6 for OT problem in $d = 1$. We consider the two cost functions $c(s_1, s_2) = (s_1 + s_2)^2$ and $c(s_1, s_2) = -(s_1 - s_2)^2$ satisfying the conditions in Proposition 3.5 (see Figures 1 and 2). μ_1 and μ_2 are chosen to be two log-normal distributions in \mathbb{R}^+ centered at $S_0 = 1$ and with variances 0.2^2 and $0.2^2 \times 1.5$. They are simulated using 2^{13} Monte-Carlo paths. For each neural network, we have used 2 hidden layers of dimension 4. We have also used a Adam stochastic gradient descent [18] with 64 minibatches for the computation of the online gradients and our algorithm has been written from scratch in C++. The exact solution has been computed using formula (9) and performing a 1d numerical integration. We have compared our algorithm with the entropy relaxation and the penalization methods outlined in Sections 2.2-2.4. We can observe that our primal-dual algorithm converges faster (to the exact solution). On one hand, the choice of the gamma factor in the penalization method is tricky. Taking a small value of γ results into convergence towards a false solution and a large γ gives noisy results. On the other hand, the entropy relaxation needs more iterations to converge. We have used in all our numerical experiments at most 10^6 iterations. For each $10^4 \times n$ iterations where n ranges from 1 up to 10^2 , we have computed the functional $J(\theta_n, \omega_n)$ by averaging over our recorded 2^{13} Monte-Carlo paths. We have also plotted the map found by our algorithm (denoted ‘‘NN’’) and compared with the Fréchet-Hoeffding solution $T(s) = F_2^{-1} \circ F_1(s)$. We found a perfect match (the blue and red curves coincide).

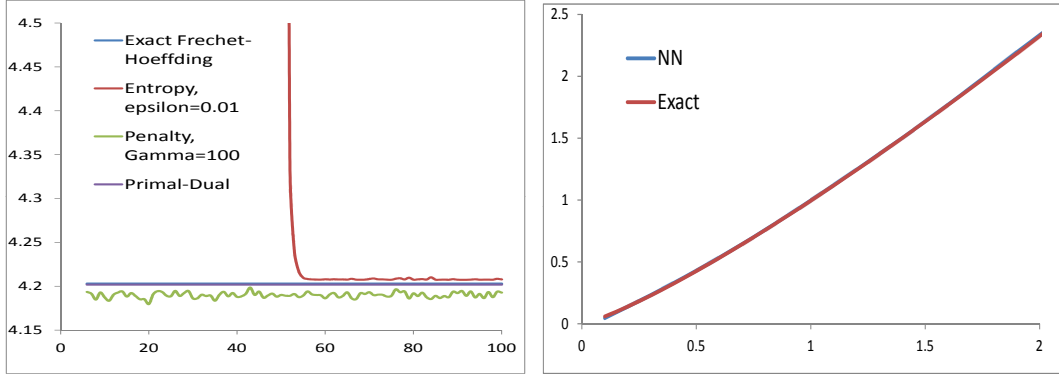


FIGURE 1. OT: $c(s_1, s_2) = (s_1 + s_2)^2$. μ_1 and μ_2 are two log-normal distributions with variances 0.2^2 and $0.2^2 \times 1.5$. Exact = 4.20. For the penalization method, we have chosen $\gamma = 100$ (similar results for $\gamma = 50, 200$). The number of iterations has been divided by 10^4 .

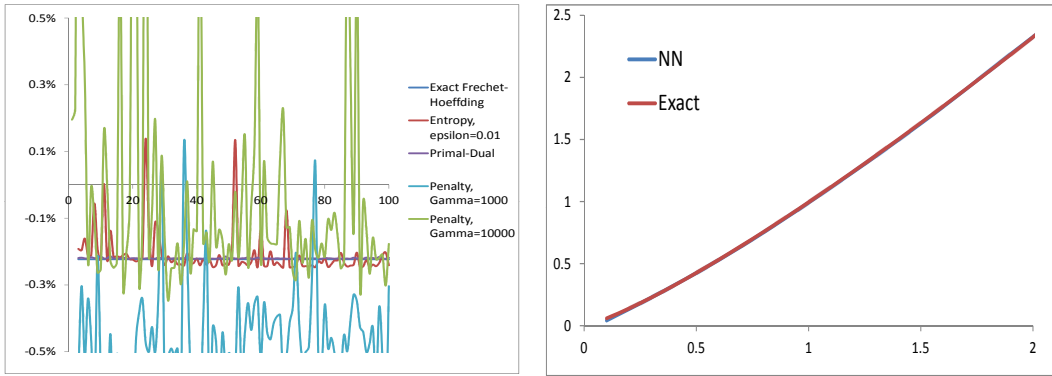


FIGURE 2. OT: $c(s_1, s_2) = -(s_1 - s_2)^2$. μ_1 and μ_2 are two log-normal distributions with variances 0.2^2 and $0.2^2 \times 1.5$. Exact = -0.22% . For the penalization method, we have chosen $\gamma = 1000, 10000$. The number of iterations has been divided by 10^4 .

4.2. 2-Wassertein distance in \mathbb{R}^d , $d = 2, 10, 20$. Next, we compute the 2-Wassertein distance in \mathbb{R}^d . In our notation, this corresponds to the payoff $c(s_1, s_2) = -\sum_{i=1}^d (s_1^i - s_2^i)^2$ with a minus sign. We have first considered $d = 2$ (see Figure 3–left). We have compared the entropy relaxation method against our primal-dual algorithm. As concluded in $d = 1$, our algorithm converges faster and the entropy relaxation method is unstable according to our choice of ϵ . For large epsilon, the Wasserstein distance is underestimated and for small epsilon, our SGD is noisy and therefore the result can not be trusted. As a consequence, the entropy relaxation method could not be used as presented for computing the Wasserstein distance. The convergence is very fast for our primal-dual method. Here μ_1 and μ_2 are chosen to be two uncorrelated *normal* distributions in \mathbb{R}^d with variances 1 and 2 for which the exact 2-Wassertein distance in \mathbb{R}^d is $\mathcal{W}_2(\mu^1, \mu^2)^2 = d(\sqrt{2} - \sqrt{1})^2$. Then, we consider only our primal-dual algorithm and take $d = 10$ and $d = 20$ (see Figure 3–right). For each neural network, we have used 1 hidden layer of dimension 50.

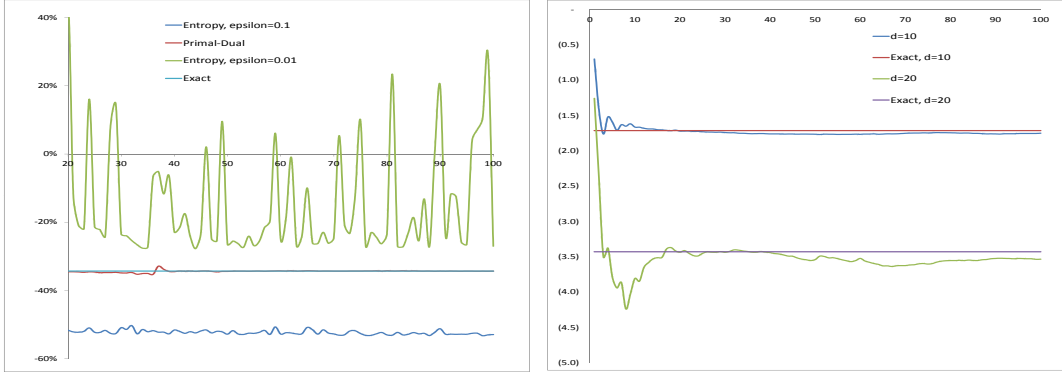


FIGURE 3. OT: $c(s_1, s_2) = -\sum_{i=1}^d (s_1^i - s_2^i)^2$. μ_1 and μ_2 are two uncorrelated normal distributions in \mathbb{R}^d with variances 1 and 2. Left: $d = 2$. The number of iterations has been divided by 10^4 . Right: $d = 10$ and $d = 20$. The number of iterations has been divided by 10^3 here as our algorithm converges quickly.

4.3. **MOT in $d = 1$.** A similar test has been performed in the case of MOT in $d = 1$ with a cost $c(s_1, s_2) = (s_1 + s_2)^3$ for which the martingale twist condition $\partial_{s_1} \partial_{s_2}^2 c > 0$ is satisfied. Our optimization converges towards the exact solution obtained using a simplex algorithm (see Figure 4).

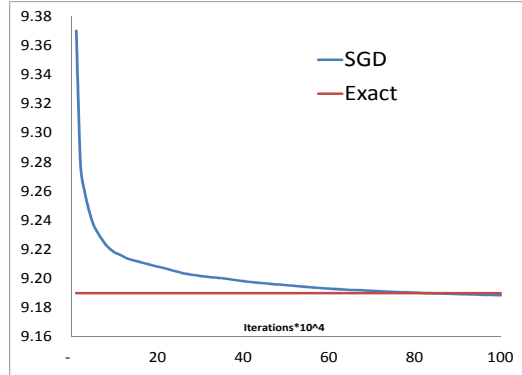


FIGURE 4. MOT: $c(s_1, s_2) = (s_1 + s_2)^3$. μ_1 and μ_2 are two log-normal distributions with variances 0.2^2 and $0.2^2 \times 1.5$ (in the convex order). Exact using a simplex: 9.19.

4.4. **Anomaly detection in $d = 2$.** As a final simple numerical example, we consider our anomaly detection algorithm outlined in Section 3.5. We have used 2 hidden layers of dimension 10. We take for μ^{real} a two-dimensional uncorrelated log-normal distribution with mean -0.02 , variance 0.04 and for μ^0 a two-dimensional uncorrelated normal distribution. Once the mapping $\hat{T}: \mathbb{R}^2 \mapsto \mathbb{R}^2$ is constructed by optimization, we generate some anomalies by drawing normal variables G in \mathbb{R}^2 and adding an anomaly factor $5 \times \text{sign}(G)$. The normal variables are generated without introducing this anomaly factor. The two-dimensional “normal” and “abnormal” variables generated are then displayed in Figure 5. As expected, the “abnormal” data live on the edge of the two-dimensional

uncorrelated log-normal distribution. However, the generative density has a smaller support than μ^{real} , highlighting that our algorithm has not yet converged.

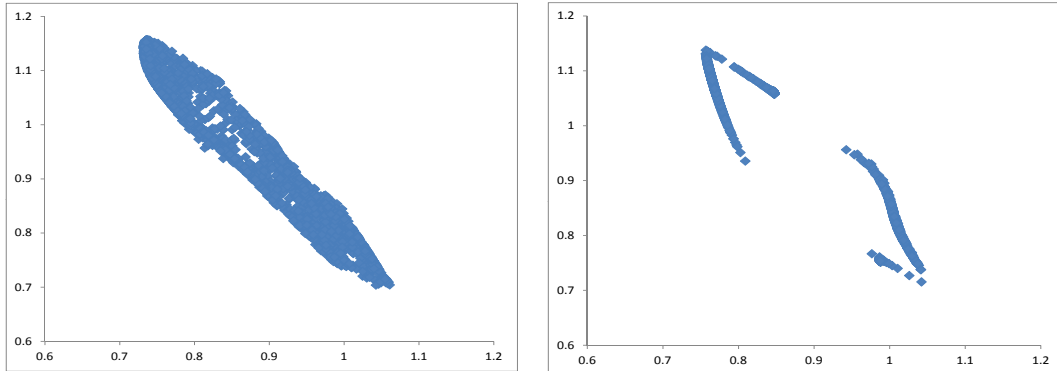


FIGURE 5. Two-dimensional normal (left) and “abnormal” (right) variables. μ^{real} is a two-dimensional uncorrelated log-normal distribution with mean -0.02 , variance 0.04 and μ^0 is a two-dimensional uncorrelated normal distribution.

REFERENCES

- [1] Arjovsky, M., Chintala, S., Bottou, L. : *Wasserstein GAN*, arXiv:1701.07875.
- [2] Beiglböck, M., Henry-Labordère, P., Penkner, F. : *Model-independent Bounds for Option Prices: A Mass-Transport Approach*, Finance and Stochastics, July 2013, Volume 17, Issue 3, pp 477–501.
- [3] Beiglböck, M., Juillet, N. : *On a problem of optimal transport under marginal martingale constraints*, Ann. Probab. Volume 44, Number 1 (2016), 42-106.
- [4] Bousquet, O., Gelly, S., Tolstikhin, I., Simon-Gabriel, C-J, Schölkopf, B. : *From Optimal Transport to Generative Modeling: the VEGAN cookbook*, arXiv:1705.07642.
- [5] Chambolle, A., Pock, T. : *A first-order primal-dual algorithm for convex problems with applications to imaging*, Journal of Mathematical Imaging and Vision, 2011.
- [6] Cuturi, M. : *Sinkhorn Distances: Lightspeed Computation of Optimal Transportation Distances*, Advances in Neural Information Processing Systems 26, pages 2292–2300, 2011.
- [7] De March, A. : *Entropic resolution for multi-dimensional optimal transport*, arxiv:181211104.
- [8] De March, A., Henry-Labordère, P. : *Building arbitrage-free implied volatility: Sinkhorn’s algorithm and variants*, arXiv:1902.04456.
- [9] De March, A. : *Local structure of multi-dimensional martingale optimal transport*, arXiv:1805.09469.
- [10] Eckstein, S., Kupper, M. : *Computation of optimal transport and related hedging problems via penalization and neural networks*, arXiv:1802.08539.
- [11] Galichon, A., Henry-Labordère, P., Touzi, N. : *A stochastic control approach to no-arbitrage bounds given marginals, with an application to Lookback options*, Ann. Appl. Probab. Volume 24, Number 1 (2014), 312–336.
- [12] Genevay, A., Cuturi, M., Peyre, G., Bach, F. : *Stochastic optimization for large scale optimal transport*, In Advances in Neural Information Processing Systems, pp. 3432–3440, 2016.
- [13] Goodfellow, I., Pouget-Abadie, J., Mirza, M., Xu, B., Warde-Farley, D., Ozair, S., Courville, A., Bengio, Y. : *Generative Adversarial Networks*, Proceedings of the International Conference on Neural Information Processing Systems (NIPS 2014). pp. 2672-2680.
- [14] Guo, G., Jan Obloj, J. : *Computational Methods for Martingale Optimal Transport problems*, Ann. Appl. Probab. (to appear), arXiv:1710.07911.
- [15] Henry-Labordère, P. : *Model-free Hedging: A Martingale optimal transportation viewpoint*, Financial Mathematics Series CRC, Chapman Hall (190 p.), 2017.
- [16] Henry-Labordère, P. : *Automated Option Pricing: Numerical Method*, Int. J. Theor. Appl. Finan., Volume 16, Issue 08, December 2013.
- [17] Henry-Labordère, P., Touzi, N. : *An Explicit Martingale Version of Brenier’s Theorem*, Finance and Stochastics, July 2016, Volume 20, Issue 3, pp 635–668.

- [18] Kingma, D.P., Ba, J. : *Adam: A Method for Stochastic Optimization*, Published as a conference paper at the 3rd International Conference for Learning Representations, San Diego, 2015. arXiv:1412.6980.
- [19] Seguy, V., Damodaran, B.B., Flamary, R., Courty, N., Rolet, A., Blondel, M. : *Large-Scale Optimal Transport and Mapping Estimation*, arXiv:1711.02283.
- [20] Villani, C. : *Topics in Optimal Transportation*, Graduate Studies in Mathematics Volume: 58; 2003.

SOCIÉTÉ GÉNÉRALE, GLOBAL MARKETS QUANTITATIVE RESEARCH

CMAP, ECOLE POLYTECHNIQUE

E-mail address: pierre.henry-labordere@sgcib.com